

Limits of validity of photon-in-cell simulation techniques

A. J. W. Reitsma and D. A. Jaroszynski

Department of Physics, University of Strathclyde, Glasgow G4 0NG, United Kingdom

(Received 20 September 2007; accepted 20 December 2007; published online 20 February 2008)

A comparison is made between two reduced models for studying laser propagation in underdense plasma; namely, photon kinetic theory and the slowly varying envelope approximation. Photon kinetic theory is a wave-kinetic description of the electromagnetic field where the motion of quasiparticles in photon coordinate-wave number phase space is described by the ray-tracing equations. Numerically, the photon kinetic theory is implemented with standard particle-in-cell techniques, which results in a so-called photon-in-cell code. For all the examples presented in this paper, the slowly varying envelope approximation is accurate and therefore discrepancies indicate the failure of photon kinetic approximation for these cases. Possible remedies for this failure are discussed at the end of the paper. © 2008 American Institute of Physics. [DOI: 10.1063/1.2834300]

I. INTRODUCTION

The study of propagation of short, intense laser pulses in underdense plasma is relevant to applications ranging from x-ray lasers¹ to particle accelerators² and radiation sources.³ At high intensities and for short duration, the evolution of optical pulses is highly nonlinear and dominated by the response of the plasma medium. This leads to interesting effects such as Raman scattering,⁴ relativistic self-focusing,⁵ and strong wakefield excitation.⁶ Under certain circumstances, the nonlinear evolution of the laser pulse leads to self-injection and acceleration of electron bunches into the plasma wake.⁷ Furthermore, there is an interesting analogy between the propagation of a relativistic electron bunch in a plasma and the evolution of a laser pulse in plasma.⁸ This analogy is most elegantly elucidated by the *photon kinetic* theory,⁹ which models the laser pulse as a collection of quasiparticles with classical position-wave number phase-space coordinates that follow the ray-tracing equations. This reduced approach, where phase-space coordinates compare with the position-momentum coordinates of relativistic electrons, allows the reinterpretation of certain aspects of laser-plasma interactions in terms of well-known beam-plasma instabilities.¹⁰ However, even though the analogies are very attractive, it is important to assess the limits of validity of the photon kinetic approach. In this paper we do so by choosing several standard problems and comparing the results of numerical simulations of laser pulse propagation using two different codes, one based on the slowly varying amplitude approximation and the other based on the photon kinetic method.

The organization of this paper is as follows. An introduction to photon kinetic theory is given in Sec. II, which is followed by a brief description in Sec. III of the numerical implementation of photon kinetic theory with a so-called photon-in-cell code. The main results of this paper are given in Sec. IV, in which four examples of simulation results with varying degrees of agreement between the envelope and the photon kinetic methods are presented. Because in all cases described here the slowly varying envelope approximation is known to be valid, any difference between the two results

implies a failure of the photon kinetic method.¹¹ Possible remedies for these failures are discussed in Sec. V and conclusions are offered in Sec. VI.

II. PHOTON KINETIC THEORY

The photon kinetic theory, which is one particular example of the so-called *wave-kinetic* theories,¹² has emerged from the phase-space formulation of quantum mechanics.¹³ This formulation employs the Wigner transform to define a phase-space density $W(x, p, t)$ from the wave function $\psi(x, t)$, as given by

$$\frac{1}{2\pi\hbar} \int_{-\infty}^{\infty} \psi(x + s/2, t) \psi^*(x - s/2, t) \exp(ips/\hbar) ds. \quad (1)$$

The phase-space density W is real, but not necessarily positive. Although W is *not* a probability density in phase space—according to Heisenberg's uncertainty principle, no such quantity can exist—it does have similar properties; for example, the integration of W over p or x yields the correct non-negative value for the probability density in position or momentum, respectively. From the Schrödinger equation one derives the following equation for the time evolution of W :

$$\frac{\partial W}{\partial t} + \frac{p}{m} \frac{\partial W}{\partial x} = \sum_{n=0}^{\infty} (-)^n \frac{\hbar^{2n}}{(2n+1)!} \frac{\partial^{2n+1} V}{\partial x^{2n+1}} \frac{\partial^{2n+1} W}{\partial p^{2n+1}}, \quad (2)$$

where $V(x, t)$ denotes the (real-valued) potential. The infinite series on the right-hand side occurs naturally as a Taylor expansion around $s=0$. In the classical limit ($\hbar \rightarrow 0$), only the $n=0$ -term on the right-hand side survives, and reduces Eq. (2) to

$$\frac{\partial W}{\partial t} + \frac{p}{m} \frac{\partial W}{\partial x} - \frac{\partial V}{\partial x} \frac{\partial W}{\partial p} = 0. \quad (3)$$

A wave-kinetic theory is what emerges when a similar reduction is performed on a classical wave theory rather than the Schrödinger equation. In addition, one usually considers the corresponding W as a continuous distribution of so-called quasiparticles rather than a phase-space probability density.

In the case of the photon kinetic theory, the following Vlasov equation is deduced from Maxwell's equations:¹⁰

$$\frac{\partial f}{\partial t} + \frac{\partial \Omega}{\partial k} \frac{\partial f}{\partial x} - \frac{\partial \Omega}{\partial x} \frac{\partial f}{\partial k} = 0 \quad (4)$$

for a distribution $f(x, k, t)$ of quasiparticles. We will simply refer to these particles as photons, although they should not be confused with photons in the quantum-mechanical sense. Furthermore, Ω is the frequency of the photon, as given by a local dispersion relation $\Omega^2(x, k, t) = c^2 k^2 + \Omega_p^2(x, t)$, where Ω_p is a generalized, space and time-varying plasma frequency. The local dispersion relation is not exact, but is an approximation similar to that producing Eq. (3) from Eq. (2). The space and time dependence of Ω_p follows from the particular model selected to describe the plasma response, several examples of which will be given below. The Vlasov equation describes the transport of f along photon trajectories, which are given by ray-tracing equations. The time variation of Ω_p results in a frequency change, an effect known as photon acceleration.¹⁴

It is clear that the concept of a single quasiparticle makes little sense, because it would be sharply localized both in coordinate x and wave number k and would violate the uncertainty principle. Thus only a distribution of quasiparticles that occupies a sufficiently large phase-space volume is allowed, as given by $\Delta x \Delta k \geq 2\pi$, which is basically the equivalent of the uncertainty relation. We should stress that a wave-kinetic theory is a *reduced* description, as it is the result of an approximation similar to the one that leads from Eq. (2) to Eq. (3). Therefore, it is important to investigate whether this reduction can be justified.

III. PHOTON-IN-CELL METHOD

The appealing mathematical elegance of the photon kinetic method has inspired several authors to construct numerical codes based on the approach.^{15–18} All of these use the photon-in-cell algorithm described below. The numerical implementation of Eq. (4) uses a Klimontovich distribution,

$$f(x, k, t) = \sum_{i=1}^N \delta[x - x_i(t)] \delta[k - k_i(t)], \quad (5)$$

of N macroparticles that are convected in a Lagrangian manner by integrating the ray-tracing equations for (x_i, k_i) . The distribution of the form of Eq. (5) results in a vector potential envelope,

$$|a|^2(x, t) = \int \frac{f(x, k, t)}{\Omega(x, k, t)} dk, \quad (6)$$

which is a collection of δ -spikes located at photon positions x_i . For a sufficiently large value of N , a smooth distribution of $|a|^2$ —corresponding to a smooth f —can be computed on a fixed (Eulerian) spatial grid using the well-known particle-in-cell method,¹⁹ which effectively gives the macroparticles a finite size. A self-consistent calculation requires the force to be recomputed on the grid at each time-step using the new $|a|^2$ -distribution. The subsequent (x_i, k_i) -update involves an interpolation of the force from the grid to the photon posi-

tions. Although this implementation is numerically straightforward, one must ensure that discrete particle effects are reduced sufficiently. This is usually done by carefully choosing the number and initial distribution of the macroparticles, and the magnitude of the time-step. It may even be necessary to introduce artificial smoothing of the force distribution (e.g., by Fourier filtering).¹⁵

IV. COMPARISON OF RESULTS

A. Channel guiding

It is sometimes argued that wave-kinetic theories lack phase information and are therefore unable to deal correctly with interference effects.¹⁷ While it is true that the wave function $\psi(x, t)$ can be reconstructed from Eq. (1), this can only be done *up to an arbitrary phase factor* that is constant in x , but may vary with t . In practice this is not a problem, because for the calculation of expectation values this arbitrary phase factor is irrelevant anyway. Another question is whether phase information is lost in the transition from Eq. (2) to Eq. (3). The naïve answer to this is “yes, of course,” because Eq. (3) describes the probability density of *classical* particles, and it is clear that these do not exhibit interference effects. However, the answer turns out to be a bit more subtle. We illustrate this by presenting a simple one-dimensional model of laser pulse guiding in a preformed plasma channel waveguide,²⁰ considering only one transverse coordinate x and time t , for simplicity. The equation for the slowly varying envelope $a(x, t)$ of the dimensionless transverse vector potential eA/mc^2 is

$$2i\omega_0 \frac{\partial a}{\partial t} + c^2 \frac{\partial^2 a}{\partial x^2} = \omega_p^2 C(x) a, \quad (7)$$

where ω_0 is the laser carrier frequency, $\omega_p^2 = 4\pi n e^2 / m$ defines a reference plasma frequency ω_p , and n is the plasma density. The function $C(x)$ defines the profile of the plasma channel. The slowly varying envelope approximation is based on the assumption $\omega_0 \gg \omega_p$ (underdense plasma). Conveniently, Eq. (7) is just the Schrödinger equation in disguise, with a playing the role of ψ and C playing the role of the potential V . If we take C to be a quadratic function $C(x) = 1 + x^2/y^2$, we obtain the exact analog of the quantum harmonic oscillator. The eigenstates of the harmonic oscillator, given by the well-known Hermite–Gaussian functions, correspond to the eigenmodes of the parabolic plasma channel. Matched propagation (i.e., without spot size oscillations) is possible for a Gaussian laser pulse $a = a_0 \exp(-x^2/2r^2)$ if the matching condition $(k_p r)^2 = k_p y$ is met (where $k_p = \omega_p / c$ defines the plasma wave number).

Now notice that for the harmonic oscillator, the transition from Eq. (2) to Eq. (3) is *exact* due to the fact that all higher-order derivatives of V vanish. Admittedly, this is a bit of a coincidence, but it leaves us wondering how the *classical* Eq. (3) can faithfully represent the *quantum* harmonic oscillator. After all, interference and other nonclassical effects do occur in the quantum harmonic oscillator. The answer to this paradox is that if the phase information is correctly encoded in the initial distribution $W(x, p, t=0)$, then letting it evolve according to Eq. (3), will produce the correct

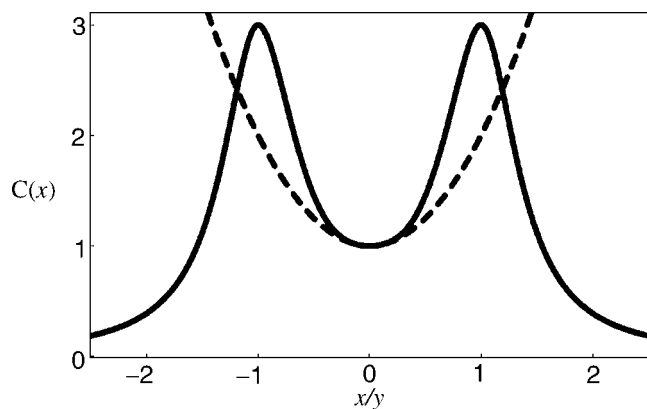


FIG. 1. Nonparabolic channel profile (solid line) and parabolic approximation (dashed line).

quantum-mechanical result for $W(x, p, t > 0)$. Interference effects typically show up as regions in phase space where W assumes negative values, which is the classically forbidden region.

Apart from checking the consistency between numerical codes, there is not much to be gained from comparing the simulation of Eq. (7) for a parabolic $C(x)$ with the corresponding photon-in-cell simulation, because they show exactly the same result, as expected. Thus, we move on to present a case where $C(x)$ has a nonparabolic profile, as shown in Fig. 1. Simulation results for an initial laser profile $a(x) = a_0 \exp(-x^2/2r^2) \exp(ik_\perp x)$ are shown in Fig. 2. The initial photon distribution is given by a discrete representation of $f(x, k_x) = \omega_0 a_0^2 \exp[-x^2/r^2 - (k_x - k_\perp)^2 r^2]$; i.e., the Wigner transform of $a(x)$. The parameters are $a_0 = 1/3$, $\omega_0/\omega_p = 20$, $k_p y = 5$, $(k_p r)^2 = k_p y$, $k_\perp = -k_p/\sqrt{2}$, corresponding to injection of the laser pulse into the waveguide at an angle of about 2° . The striking qualitative difference between the envelope and photon kinetic simulation results shows clearly the importance of the higher-order derivatives of C on the evolution of $|a|^2$. The result of the photon kinetic simulation can be understood as phase-mixing of a distribution of particles in an anharmonic potential, while the most natural interpretation of the envelope simulation results is a beating of several eigenmodes of the channel. Because these modes are close to the “ground state” (in the quantum sense), the system is much closer to the “quantum limit” than the “classical limit,” and therefore it is not surprising to see a big difference between photon kinetic and envelope simulation results.

B. Relativistic self-focusing

We can also use the one-dimensional model introduced above to describe the propagation of a laser pulse in a uniform plasma, but including relativistic self-focusing.⁵ In this case, the function $C[a(x)] = (1 + |a|^2)^{-1/2}$ is defined self-consistently in terms of the vector potential envelope rather than prescribed as a function of x . The dependence of C on a arises from the relativistic mass increase of the plasma electrons due to the quiver motion. For simplicity, we neglect the contribution to self-focusing from the electron density

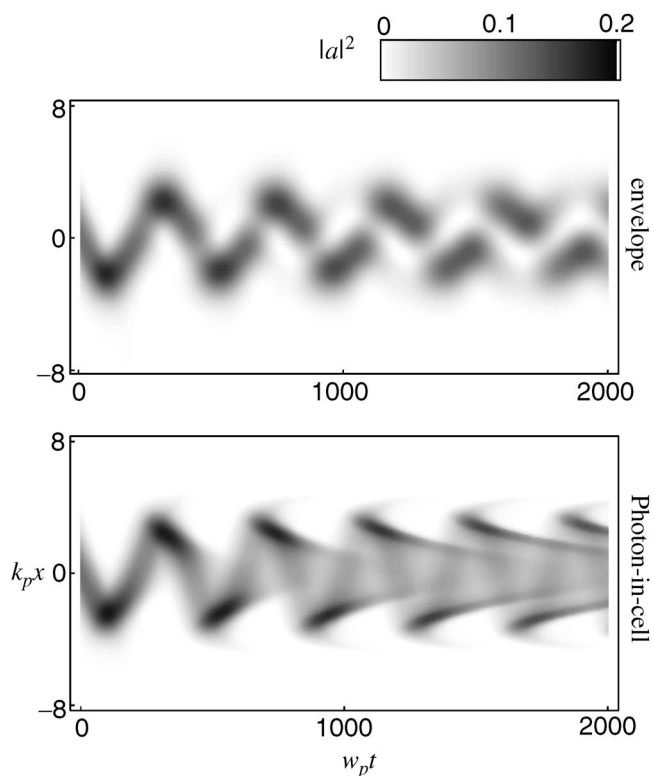


FIG. 2. Evolution of spatial envelope from simulation of propagation in nonparabolic channel.

perturbation or wake excited by the ponderomotive force of the laser pulse.⁵ In Fig. 3 we compare the results of envelope and photon kinetic simulations for $a_0 = 2.4$, $(k_p r)^2 = 15$. The dramatic difference is due to the dependence of C on a ,

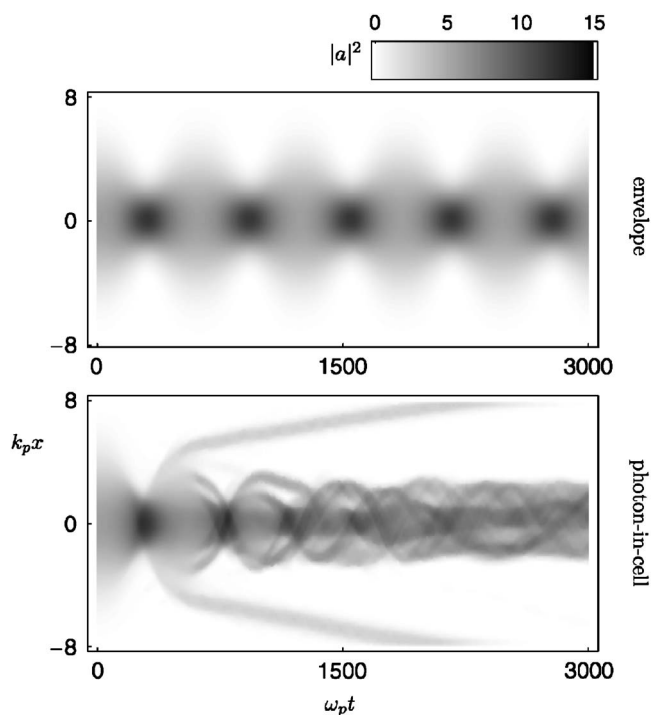


FIG. 3. Evolution of spatial envelope from simulation of relativistic self-focusing in uniform plasma.

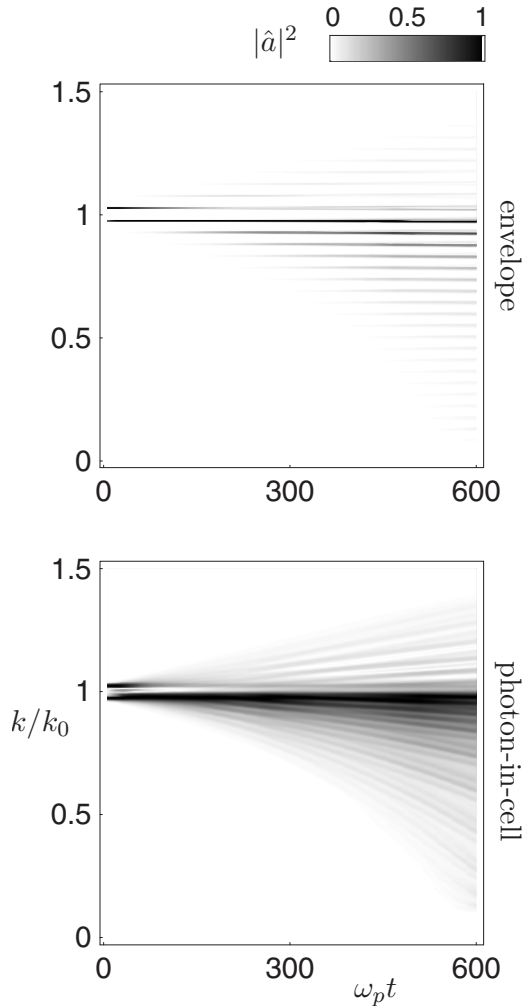


FIG. 4. Spectral evolution from forward Raman scattering simulation. The spectra are normalized by the maximum over k at each time-step.

which sets up a feedback loop in the system, that in turn leads to rapid growth of small differences between the two approximations.

As an important aside, we note that the only allowed choice of the initial photon distribution is the Wigner transform of the vector potential. In earlier work on photon-in-cell simulations, Tappert *et al.*¹⁵ used an initial photon distribution that, up to a normalization constant, is equal to $f_a(x, k_x) = [k_x^2 - k_p^2 |a|^2(x)/2]^{1/2}$ when the quantity between brackets is non-negative, and 0 otherwise. They used this distribution to model a spatial envelope soliton²¹ $a(x, t) = a_0 \exp(i\lambda t) \text{sech}(a_0 k_p x/2)$ with $\lambda = \omega_p^2(a_0^2/4 - 1)/2\omega_0$, which is an exact solution of the envelope equation (7) in the limit of small amplitude, where $C[a(x)] \approx 1 - |a|^2/2$. The reason that the photon-in-cell code produces a stable $|a|^2$ -profile with f_a as an initial distribution is that f_a is, by construction, constant along the ray-tracing trajectories; therefore, it should produce a stable envelope solution for *any* given profile of $|a|^2$, which is clearly unphysical. The sech profile gives a stable envelope as an initial condition for the envelope code, but its Wigner transform and the photon-in-cell code diverges considerably.

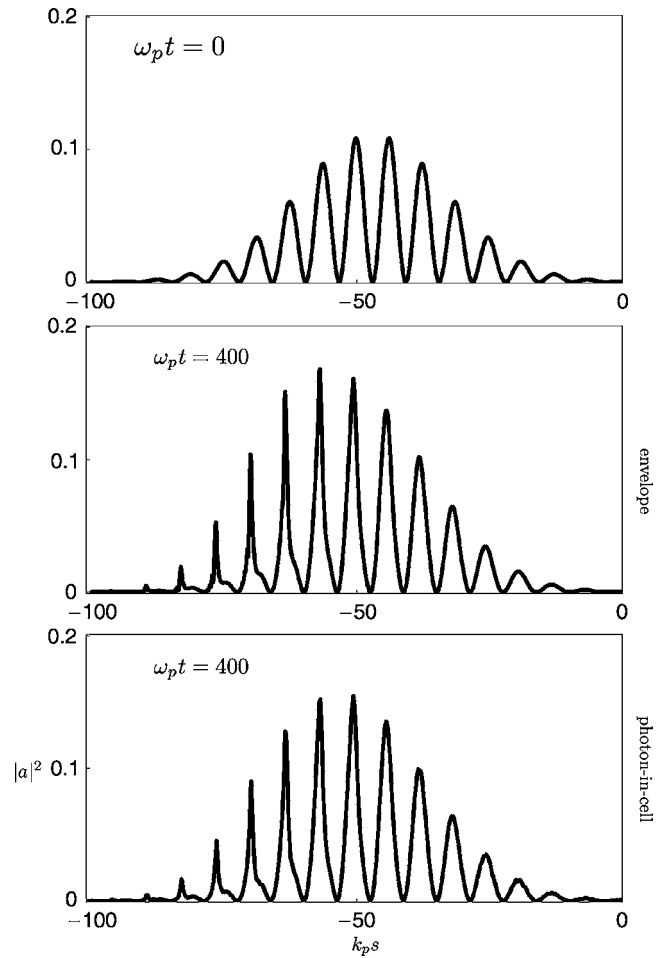


FIG. 5. Snapshots of spatial envelope from forward Raman scattering simulation.

C. Long pulse with resonant beat-wave

We now discuss examples of longitudinal laser pulse evolution using a simple one-dimensional model, relevant to laser wakefield acceleration. The envelope equation becomes

$$2i\omega_0 \frac{\partial a}{\partial t} + 2c \frac{\partial^2 a}{\partial s \partial t} = \frac{\omega_p^2}{1 + \phi} a, \quad (8)$$

where ϕ denotes the dimensionless electrostatic potential describing the laser wakefield, and $s = z - ct$ is a longitudinal coordinate moving at the speed of light. In the above equation, the mixed derivative takes into account the spectral changes of the laser pulse and energy coupling between the laser pulse and the wakefield.²² The wakefield is calculated using the quasistatic approximation⁶

$$\frac{\partial^2 \phi}{\partial s^2} = \frac{k_p^2}{2} \left[\frac{1 + |a|^2}{(1 + \phi)^2} - 1 \right]. \quad (9)$$

In the first example that we discuss, the initial condition is $a(s) = a_0 \cos(k_p s/2) \exp(-s^2/2l^2)$, which represents the sum of two perfectly overlapping laser pulses with central wave numbers $k_{\pm} = k_0 \pm k_p/2$. The interference between these pulses produces a beat-wave pattern that is modulated at the plasma frequency and resonantly drives the wakefield. The

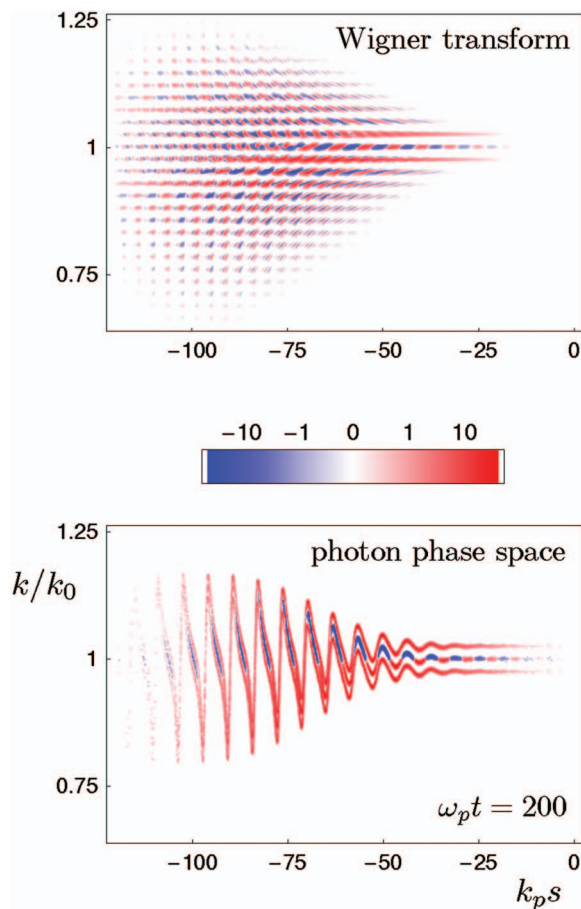


FIG. 6. (Color) Snapshots of Wigner transform and photon phase space from forward Raman scattering simulation.

feedback of the wakefield on the pulse evolution results in a resonant coupling to other laser wave numbers separated by multiples of the plasma wave number, in other words it induces a cascade of forward Raman scattering.²³ This scattering cascade is clearly visible in the simulation results shown in Fig. 4, as contour plots of the Fourier spectrum $|\hat{a}|^2(k, t)$, where $\hat{a}(k, t)$ denotes the spatial Fourier transform of $a(s, t)$. Other parameters for the simulation are $a_0 = 1/3$, $k_p l = 20$. Figure 4 shows instantaneous coupling to the Stokes and, to a lesser extent, the anti-Stokes sidebands. The corresponding evolution of the spatial envelope $|a|^2(s, t)$ is illustrated in Fig. 5, which shows the initial envelope profile and two snapshots at $\omega_p t = 400$, one from the envelope code and one from the photon-in-cell code.

The significance of the beat-wave example is to highlight the role of interference effects. The initial photon distribution corresponding to $a(s)$ is $f(z, k_z) = \omega_0 a_0^2 e^{-z^2/l^2} \times [e^{-(k_z - k_+)^2 l^2} + e^{-(k_z - k_-)^2 l^2} + 2 \cos(k_p z) e^{-(k_z - k_0)^2 l^2}]$, which consists of three ensembles of photons, two corresponding to the respective laser pulses and one representing the beat-wave pattern.¹⁷ The third ensemble has regions where f assumes negative values. The results of the photon-in-cell simulation with the above f as initial condition are shown alongside the envelope simulation results in Figs. 4 and 5. Figure 4 shows clearly that the spectral evolution is completely different.

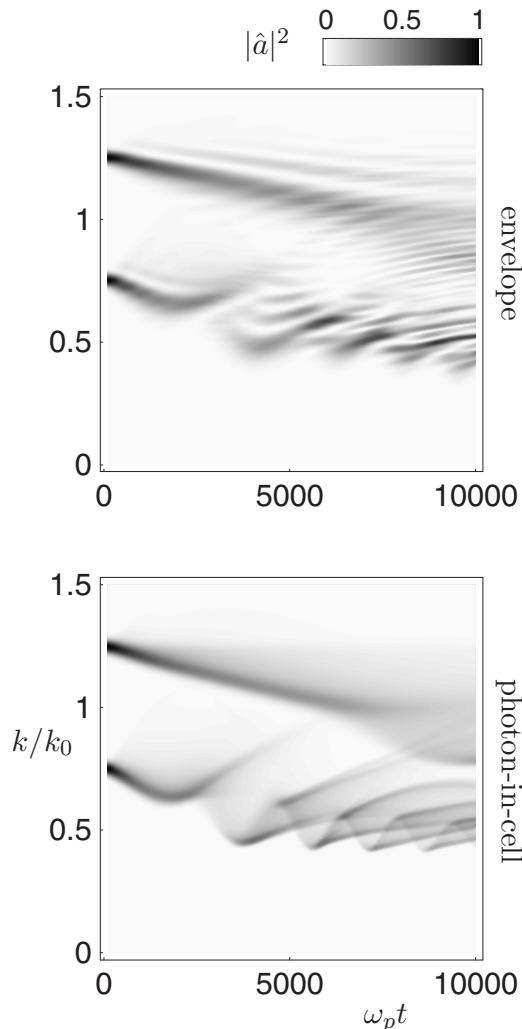


FIG. 7. Spectral evolution from split-pulse simulation. The spectra are normalized by the maximum over all k and t .

This is expected, as the photon trajectories are given by the ray-tracing equations: This means that the photon wave number spectrum can only change in a continuous way, i.e., without instantaneous coupling to sidebands. Therefore, unlike the case of a parabolic plasma channel, phase information in the photon kinetic approximation case does not propagate correctly, although it is correctly encoded in the initial distribution. Nonetheless, the photon-in-cell code does remarkably well in reproducing the spatial profile of the envelope code, as seen in Fig. 5. A useful illustration of the difference between envelope and photon-in-cell codes is a comparison of the Wigner transform of the envelope with the photon phase space of the photon-in-cell code, as given by the snapshot shown in Fig. 6. The photon phase-space plot confirms that the mechanism of frequency modulation in the photon-in-cell simulation is photon acceleration and deceleration of the three initial photon ensembles, whereas the frequency modulation in the envelope simulation is attributed to the creation of more photon ensembles that are separated from the initial ones by multiples of the plasma wavenumber.

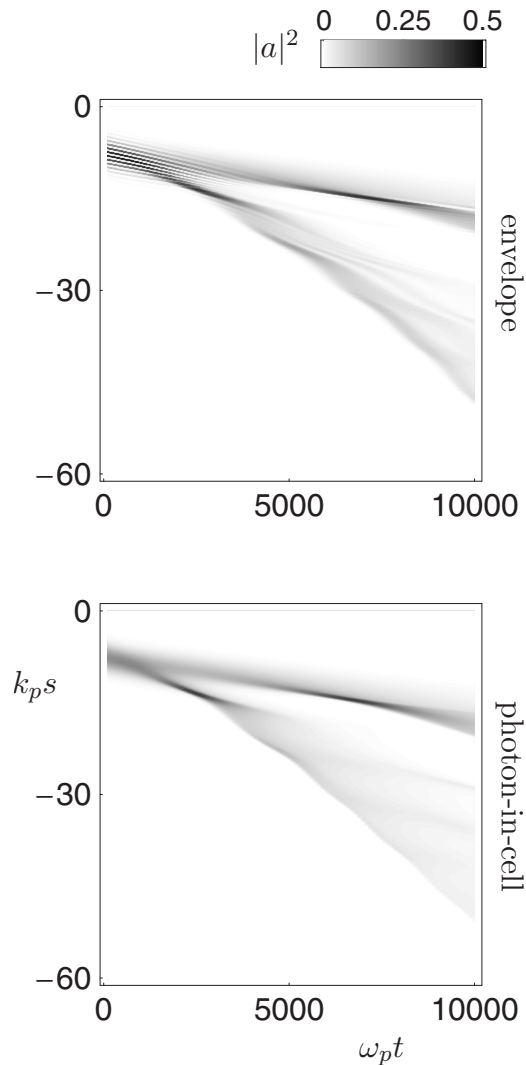


FIG. 8. Evolution of spatial envelope from split-pulse simulation.

D. Short pulse with off-resonant beat-wave

The last example we discuss is a repeat of the previous case, but now with $k_{\pm} = k_0 \pm k_0/4$. The results of the envelope and photon-in-cell simulations with parameters $a_0 = 2/3$, $k_p l = 2$ are shown in Figs. 7–9. The spectral evolution now shows only qualitative agreement, but the spatial envelopes still compare quantitatively rather well, except for an absence of the envelope modulation feature in the photon-in-cell simulations. These differences arise because the third ensemble of photons has been omitted from the initial photon distribution. This is justified on the grounds that the beat-wave interference pattern is modulated at a period much shorter than the plasma wavelength, which is far from resonance and, hence, very ineffective in exciting a plasma wave. It is observed that the laser pulses, which are initially perfectly overlapping, become separated at later times due to the difference in group velocity. The leading pulse, consisting of photons with initial wave number close to k_+ , is continually red-shifted as it excites a wakefield, while the trailing pulse, consisting of photons with initial wave number close to k_- , is both red-shifted and blue-shifted as it slips backward through several wave buckets of the wakefield excited by the leading

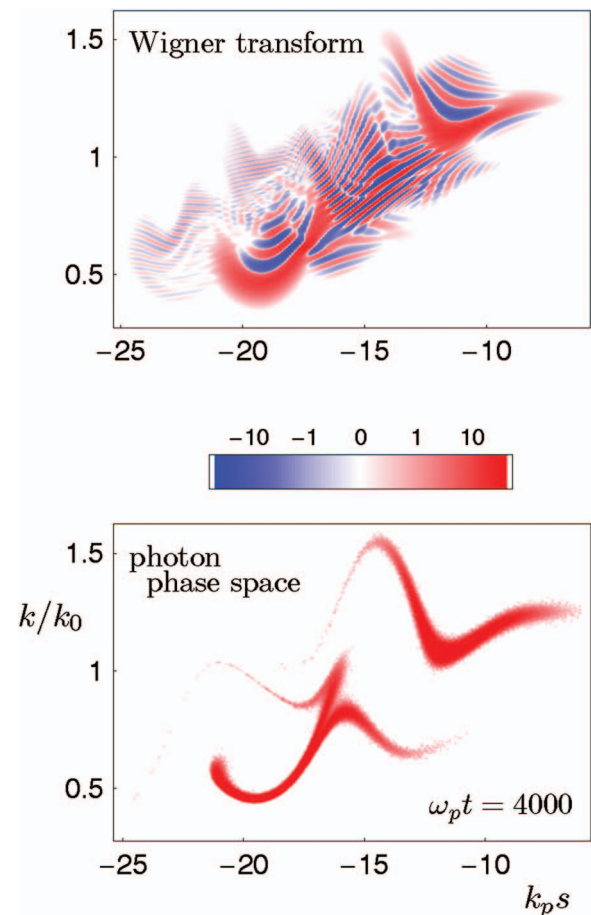


FIG. 9. (Color) Snapshots of Wigner transform and photon phase space from split-pulse simulation.

pulse. The simulations indicate that the photon kinetic method is adequate in describing these phenomena. The comparison between snapshots of the photon phase-space plot and the Wigner transform, as presented in Fig. 9, shows that the evolution of regions with high photon concentration (which have a deep red color) compares favorably.

V. DISCUSSION

We now discuss possible ways to remedy the failures of the photon kinetic method that we have uncovered in this paper. The root cause of these failures is the omission of higher-order terms in the approximation in deriving Eq. (3) from Eq. (2). We suggest that an obvious solution would be to include several or all of these higher-order terms. However, the resulting equations are not as easily amenable to numerical implementation as Eq. (4). In particular, the photon-in-cell method based on ray-tracing (method of characteristics) becomes difficult to implement as the higher-order terms are effectively *nonlocal* operators in k -space, which the forward Raman scattering example clearly illustrates. Another way to see this is to note that the infinite series on the right hand side of Eq. (2) can be rewritten²⁴ as an integral $\int K(x, q, t) W(x, p+q, t) dq$ that involves coupling between different momenta, where the kernel $K(x, q, t)$ depends on the potential $V(x, t)$. An alternative to the photon-

in-cell method is the Vlasov–Fokker–Planck approach where a continuous f is defined on a phase-space grid. This is computationally very costly and may not be viable, especially when envelope or full wave codes are more economical. As an example, consider an implementation of the integral formula given above, which has the obvious advantage of including all higher-order terms, which would require evaluating a double integral *for each grid point at each time-step*. Finally, it should be noted that all the examples given in this paper fall in the category where the slowly varying envelope approximation is valid. This excludes a number of important effects in intense laser-plasma interaction, such as backward Raman scattering. Recently, a generalization of photon kinetic theory has been introduced²⁵ that is formally equivalent to the full wave dynamics for electromagnetic waves in plasma, and therefore includes all of these effects. Whether this generalized photon kinetic theory is amenable to numerical modelling is, at present, unclear.

VI. CONCLUSION

We have studied the slowly varying envelope and photon kinetic approximations for laser pulse propagation in underdense plasma by comparing the results of numerical simulations based on envelope and photon-in-cell codes. The envelope codes are known to give the correct result for all the examples given in this paper. Thus, any discrepancies imply a failure of the photon kinetic theory. We have seen that for laser pulse propagation in a nonparabolic plasma channel and for relativistic self-focusing in a uniform plasma, the photon kinetic code does not reproduce the correct spatial envelope profile. In the case of two overlapping pulses producing a resonant beat-wave, the photon kinetic code reproduces the correct spatial profile, but does not describe the spectrum correctly. In the case of two short overlapping pulses producing an off-resonant beat-wave, the photon kinetic code compares well with the envelope code producing spatial envelopes that agree quantitatively. However, the spectral evolution only agrees qualitatively in this case. It is remarkable that such good qualitative agreement is produced in spite of leaving out the beat-wave information from the initial photon distribution. The discrepancies found above are attributed to the truncation of an infinite series of higher-

order terms in a Taylor expansion, and are possibly remedied by inclusion of one or more of these higher-order terms.

- ¹J. J. Rocca, V. Shlyaptsev, F. G. Tomasel, O. D. Cortázar, D. Hartshorn, and J. L. A. Chilla, Phys. Rev. Lett. **73**, 2192 (1994).
- ²T. Tajima and J. M. Dawson, Phys. Rev. Lett. **43**, 267 (1979).
- ³D. A. Jaroszynski, R. Bingham, E. Brunetti, B. Ersfeld, J. Gallacher, B. van der Geer, R. Issac, S. P. Jamison, D. Jones, M. de Loos, A. Lyachev, V. Pavlov, A. Reitsma, Y. Saveliev, G. Vieux, and S. M. Wiggins, Philos. Trans. R. Soc. London, Ser. A **364**, 689 (2006).
- ⁴W. B. Mori, C. D. Decker, D. E. Hinkel, and T. Katsouleas, Phys. Rev. Lett. **72**, 1482 (1994).
- ⁵B. Hafizi, A. Ting, P. Sprangle, and R. F. Hubbard, Phys. Rev. E **62**, 4120 (2000).
- ⁶A. Ting, E. Esarey, and P. Sprangle, Phys. Fluids B **2**, 1390 (1990).
- ⁷A. Pukhov and J. Meyer-ter-Vehn, Appl. Phys. B **74**, 355 (2002).
- ⁸A. Reitsma and D. Jaroszynski, Philos. Trans. R. Soc. London, Ser. A **364**, 635 (2006).
- ⁹L. O. Silva and J. T. Mendonça, Phys. Rev. E **57**, 3423 (1998).
- ¹⁰N. L. Tsintsadze and J. T. Mendonça, Phys. Plasmas **5**, 3609 (1998).
- ¹¹We have checked that it is actually the photon kinetic method that breaks down, not our code.
- ¹²S. W. McDonald, Phys. Rep. **158**, 337 (1988).
- ¹³E. Wigner, Phys. Rev. **40**, 749 (1932).
- ¹⁴S. C. Wilks, J. M. Dawson, W. B. Mori, T. Katsouleas, and M. E. Jones, Phys. Rev. Lett. **62**, 2600 (1989).
- ¹⁵F. D. Tappert, W. J. Cole, R. H. Hardin, and N. J. Zabusky, Bell Laboratories Memorandum PCP-79-29, in *Proceedings of the Fourth Conference on Numerical Simulations of Plasmas*, Washington, D.C., November 1970, edited by J. Boris and R. Shanny (Office of Naval Research, Arlington, 1971), p. 196.
- ¹⁶L. O. Silva, W. B. Mori, R. Bingham, J. M. Dawson, and T. M. Antonsen, Jr., IEEE Trans. Plasma Sci. **28**, 1128 (2000).
- ¹⁷A. J. W. Reitsma, R. M. G. M. Trines, R. Bingham, R. A. Cairns, J. T. Mendonça, and D. A. Jaroszynski, Phys. Plasmas **13**, 113104 (2006).
- ¹⁸C. D. Murphy, R. Trines, J. Vieira, A. J. W. Reitsma, R. Bingham, J. L. Collier, E. J. Divall, P. S. Foster, C. J. Hooker, A. J. Langley, P. A. Norreys, R. A. Fonseca, F. Fiuza, L. O. Silva, J. T. Mendonça, W. B. Mori, J. G. Gallacher, R. Viskup, D. A. Jaroszynski, S. P. D. Mangles, A. G. R. Thomas, K. Krushelnick, and Z. Najmudin, Phys. Plasmas **13**, 033108 (2006).
- ¹⁹C. K. Birdsall and A. B. Langdon, *Plasma Physics via Computer Simulation* (Adam Hilger, Bristol, 1991).
- ²⁰D. Spence and S. Hooker, Phys. Rev. E **63**, 015401 (2000).
- ²¹In fact, they investigated a temporal rather than a spatial soliton, but the same criticism applies.
- ²²S. V. Bulanov, I. N. Inovenkov, V. I. Kirsanov, N. M. Naumova, and A. S. Sakharov, Phys. Fluids B **4**, 1935 (1992).
- ²³S. Kalmykov and G. Shvets, Phys. Rev. E **73**, 046403 (2006).
- ²⁴D. F. Styer, M. S. Balkin, K. M. Becker, M. R. Burns, C. E. Dudley, S. T. Forth, J. S. Gaumer, M. A. Kramer, D. C. Oertel, L. H. Park, M. T. Rinkoski, C. T. Smith, and T. D. Wotherspoon, Am. J. Phys. **70**, 288 (2002).
- ²⁵J. P. Santos and L. O. Silva, J. Math. Phys. **46**, 102901 (2005).